

AC electrical properties of sol-gel-derived glasses in the Sb_2O_3 - SiO_2 system

This article has been downloaded from IOPscience. Please scroll down to see the full text article.

1992 J. Phys.: Condens. Matter 4 1783

(<http://iopscience.iop.org/0953-8984/4/7/016>)

View [the table of contents for this issue](#), or go to the [journal homepage](#) for more

Download details:

IP Address: 171.66.16.159

The article was downloaded on 12/05/2010 at 11:18

Please note that [terms and conditions apply](#).

AC electrical properties of sol–gel-derived glasses in the Sb_2O_3 – SiO_2 system

A Datta, Anit K Giri and D Chakravorty

Indian Association for the Cultivation of Science, Jadavpur, Calcutta-700 032, India

Received 16 July 1991, in final form 27 September 1991

Abstract. Measurements of AC resistivity have been carried out on sol–gel-derived glasses in the system $x\text{Sb}_2\text{O}_3$ – $(1-x)\text{SiO}_2$ with $x = 0.07$ and 0.23 for frequencies from 2 kHz to 100 kHz in the temperature range 80–400 K. The AC resistivities show a sharp minimum at around 310 K. This is ascribed to a reduction in the ratio of $[\text{Sb}^{5+}]$ to $[\text{Sb}^{3+}]$ in these glasses as a function of temperature. Another minimum is observed at temperatures of 178 K and 209 K for glasses 1 and 2, respectively. The frequency exponent s for AC resistivity also shows a maximum as a function of temperature at around these temperatures. The correlated barrier hopping model has been used to explain the trend of s in the temperature range 170–290 K whereas the overlapping long polaron tunnelling mechanism appears to give the correct variation in the temperature range 100–170 K. Both the glasses show anomalously large values of dielectric constant in the range 1000–6000 at a frequency of 2 kHz at around 310 K. Analyses of all these data indicate that there are antimony-rich and antimony-deficient layers present in this glass system.

1. Introduction

Oxide glasses containing transition-metal ions have been extensively studied because of their semiconducting properties (Murawski *et al* 1979, Hirashima *et al* 1987). The latter arise due to the presence of variable valence ions such as V^{4+} – V^{5+} , Fe^{2+} – Fe^{3+} and Cu^+ – Cu^{2+} within the oxide glass matrix. A strong electron–phonon interaction in these systems results in the formation of small polarons. The transport properties of these glasses are controlled by the hopping of small polarons between the low- and the high-valence sites of the transition-metal ions. The presence of Sb_2O_3 or As_2O_3 in silicate glasses leads to interesting electrical behaviour at a temperature of around 300 K. Electrical conduction in these glasses below 300 K has been shown to arise owing to the hopping of a pair of electrons (bipolarons) between ion sites having different valencies i.e. Sb^{3+} – Sb^{5+} and As^{3+} – As^{5+} (Chakravorty *et al* 1979, Kumar and Chakravorty 1980). In melt-quenched glasses which have been studied mostly so far the $[\text{Sb}^{5+}]/[\text{Sb}^{3+}]$ or $[\text{As}^{5+}]/[\text{As}^{3+}]$ ratio has been found to have values ranging from 0.03 to 0.36. On the other hand our recent work indicates that it is possible to retain a much higher fraction of arsenic ions in the pentavalent state when the glass in the As_2O_3 – SiO_2 system is prepared by the sol–gel route (Datta *et al* 1991). Such sol–gel-derived glasses have shown an interesting dielectric behaviour. We have now prepared glasses in the Sb_2O_3 – SiO_2 system using the sol–gel technique. The AC electrical behaviour is found to be interesting. We describe the details of these results in this paper.

Table 1. Compositions of the glasses studied and some of their physical parameters.

Glass	SiO ₂ (mol%)	Sb ₂ O ₃ (mol%)	Density (g cm ⁻³)	Antimony concentration N_t (cm ⁻³)	Average intersite separation R (Å)
1	92.9	7.1	2.11	2.4×10^{21}	7.5
2	76.7	23.3	2.69	6.6×10^{21}	5.3

2. Experimental details

The starting compositions for the two glasses investigated are 10 Sb₂O₃-90 SiO₂ and 30 Sb₂O₃-70 SiO₂ (in mole per cent), respectively. The final compositions as determined by chemical analyses are, however, markedly different from the above and the relevant values are summarized in table 1. It is evident that the final compositions are substantially different from the starting values. Such a difference arises because of the loss of some of the antimony ions by volatilization during the heat treatment schedule. The sol in the present case has been prepared by mixing a solution of SbCl₃ in hydrochloric acid with another of silicon tetraethoxide in ethyl alcohol. The former is made by treating the required amount (a few grams) of analytical grade Sb₂O₃ in about 10 cm³ of hydrochloric acid at room temperature and the latter is obtained by mixing about 2 cm³ of Si(OC₂H₅)₄ in 10 cm³ of ethyl alcohol, both the solutions being stirred continuously for about 10 min. It should be noted that the exact amounts of Sb₂O₃ and Si(OC₂H₅)₄, respectively, are determined by the target composition of the glass sample mentioned as above. About 2 cm³ of distilled water is added to the mixture and the resulting solution is stirred at room temperature for 30 min. The sol is allowed to gel in a Petri dish for 4-5 d. The gel is kept at 323 K for 2 d after which it is heated at a rate of about 1 K min⁻¹ to a temperature of 773 K where it is held for 2 h before being cooled to room temperature. The densities of the glasses prepared are measured by the Archimedes principle using acetone as the liquid. The density values are given in table 1.

To estimate the amount of trivalent antimony, 0.5 g of the glass sample is dissolved in a mixture of 2 cm³ of HF, 5 cm³ of HClO₄ and 5 cm³ of distilled water in a Teflon beaker and digested for 10 min. Water is added and the solution stirred with excess H₃BO₃ for 10 min, keeping its pH value at nearly unity. The solution is now titrated with 0.01 N KMnO₄ (Close *et al* 1958). To determine the pentavalent antimony content, 0.5 g of the glass sample is dissolved in a mixture of HF, H₂SO₄ and distilled water and digested for 10 min. After water has been added, the solution is stirred with excess H₃BO₃ for 10 min. The pH of the solution is brought to about unity by the addition of H₂SO₄. About 5 g of potassium iodide is added to the solution. A small amount of sodium bicarbonate is dissolved in the mixture to create an atmosphere of CO₂. The resulting solution is titrated with 0.02 N sodium thiosulphate using starch solution as an indicator (Vogel 1978). Table 2 summarizes the value of the [Sb⁵⁺]/[Sb³⁺] ratio as obtained by the above chemical analysis for the two glasses studied. In the last column of this table we show the values of this ratio for glasses as determined immediately after heat treatment of the specimens at 353 K for ½ h. The concentrations N_t of antimony ions in the two glasses have been calculated using the chemically analysed values of the total antimony and the experimentally determined densities. The average intersite separation R is calculated from the relation

Table 2. $[Sb^{5+}]/[Sb^{3+}]$ ratios for the two glasses.

Glass	$[Sb^{5+}]/[Sb^{3+}]$	
	As prepared	After heating at 353 K for $\frac{1}{2}$ h
1	1.12	0.23
2	0.92	0.43

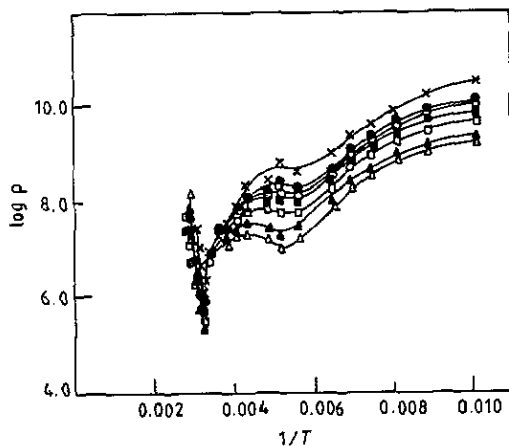


Figure 1. AC resistivity as a function of temperature for glass 1: \times , 2 kHz; \bullet , 5 kHz; \circ , 7 kHz; \blacksquare , 10 kHz; \square , 20 kHz; \blacktriangle , 50 kHz; \triangle , 100 kHz.

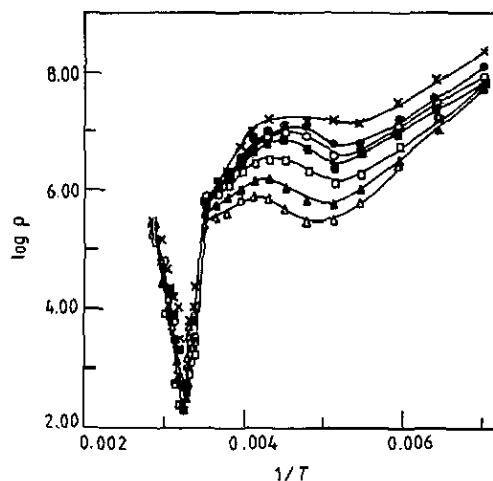


Figure 2. AC resistivity as a function of temperature for glass 2: \times , 2 kHz; \bullet , 5 kHz; \circ , 7 kHz; \blacksquare , 10 kHz; \square , 20 kHz; \blacktriangle , 50 kHz; \triangle , 100 kHz.

$$R = (1/N_i)^{1/3}. \quad (1)$$

Values of N_i and R for the two glasses are shown in the last two columns of table 1.

Electrical measurements have been carried out on specimens of about 0.4 mm thickness and having an area of about 0.5 cm². Vacuum-deposited gold films on both faces of a sample act as the electrodes. The specimen holder used is similar to that described earlier (Chakravorty *et al* 1979). The AC impedance measurements are carried out in a General Radio 1615-A capacitance bridge over a frequency range from 2 kHz to 100 kHz. Measurements are made in the temperature range 80–400 K with a stability of ± 0.5 K.

3. Results

Figures 1 and 2 show the variation in AC resistivity as a function of temperature at different frequencies for glasses 1 and 2, respectively. Both these figures show two minima in the resistivity–temperature plots. For glass 1 the minima occur at temperatures of around 309 K and 175 K and for glass 2 the corresponding temperatures are 310 K and 204 K. The resistivity values in these samples are spread over the range 10^4 – 10^{10} Ω cm in the temperature interval investigated here. It is also observed that the resistivity decreases as the antimony content in the glass is increased. Figure 3 gives the

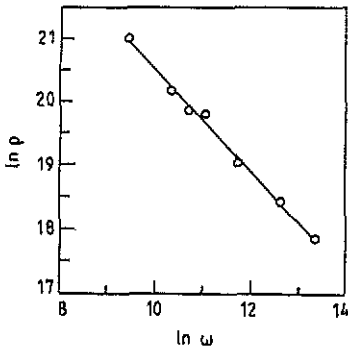


Figure 3. AC resistivity as a function of frequency for glass 2 at 183 K.

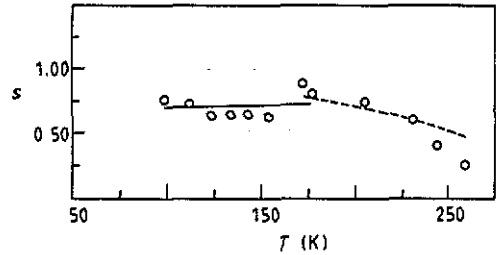


Figure 4. Variation in s as a function of temperature for glass 1: —, OLP model; ----, CBH model.

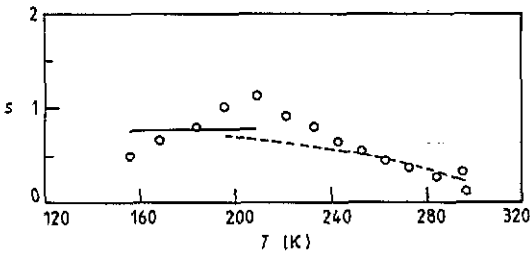


Figure 5. Variation in s as a function of temperature for glass 2: —, OLP model, ----, CBH model.

variation in AC resistivity as a function of frequency for glass 2 at 183 K. The plot is typical of both the glasses at different temperatures. It is evident that the resistivity in these glasses obeys the relation

$$\rho(\omega) \propto \omega^{-s}. \quad (2)$$

The values of s for the two glasses at different temperatures have been determined by the least-squares fitting of experimental data to the above equation. In figures 4 and 5 are shown the variation in s as a function of temperature for glasses 1 and 2, respectively. The curves show a maximum at a certain temperature, the value of the latter for glasses 1 and 2 being 178 K and 209 K, respectively. It is interesting to note that these temperatures are almost identical with those corresponding to the second minima in the resistivity-temperature plots as shown in figures 1 and 2, respectively. The data therefore indicate that the AC resistivity behaviour in these glasses is controlled by two different mechanisms in the temperature range 100–280 K. The probable physical models which explain this behaviour are discussed in the following section.

The dielectric permittivity of the present glasses shows an anomalous trend as should be evident from figures 6 and 7 which correspond to glasses 1 and 2, respectively. Figures 6(a) and 7(a) represent the variation in dielectric constant as a function of temperature whereas figures 6(b) and 7(b) show the variation in dissipation factor ($\tan \delta$) as a function of temperature for the two glasses, respectively, at different frequencies. There is a sharp peak in the value of the dielectric constant for both glasses at around 310 K with a corresponding maximum in the value of the dissipation factor. The maximum value of the dielectric constant is seen to be around 800 and 6000 at a frequency of 2 kHz for glasses 1 and 2, respectively. There is a large dispersion of the dielectric constant value as a function of frequency, the lowest values being 40 and 200, respectively, for these

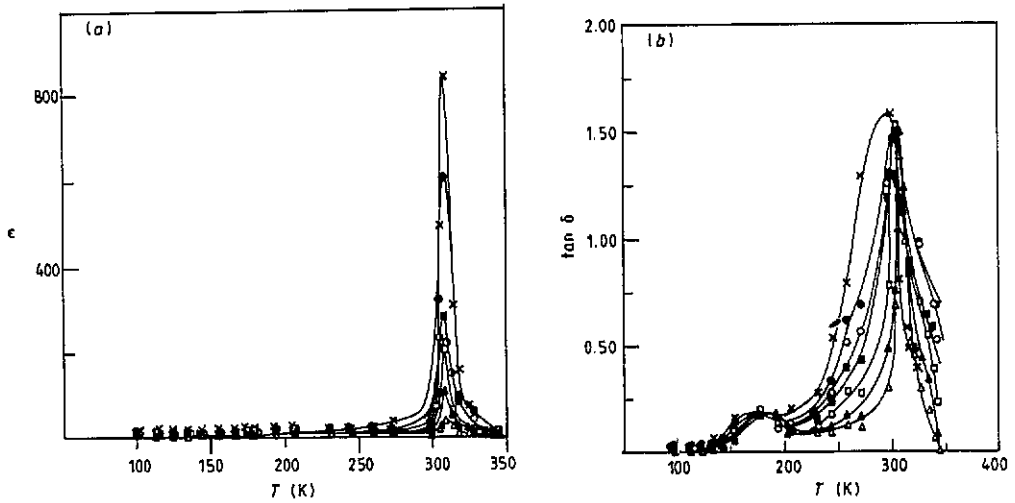


Figure 6. (a) Variation in dielectric constant as a function of temperature for glass 1: \times , 2 kHz; \bullet , 5 kHz; \circ , 7 kHz; \blacksquare , 10 kHz; \square , 20 kHz; \blacktriangle , 50 kHz; \triangle , 100 kHz. (b) Variation in $\tan \delta$ as a function of temperature for glass 1: \times , 2 kHz; \bullet , 5 kHz; \circ , 7 kHz; \blacksquare , 10 kHz; \square , 20 kHz; \blacktriangle , 50 kHz; \triangle , 100 kHz.

glasses at a frequency of 100 kHz. The temperature corresponding to the peak value of dielectric constant appears to be identical with that at which the first minimum in the resistivity-temperature plots arises, as depicted in figures 1 and 2. A possible mechanism is discussed in the subsequent section.

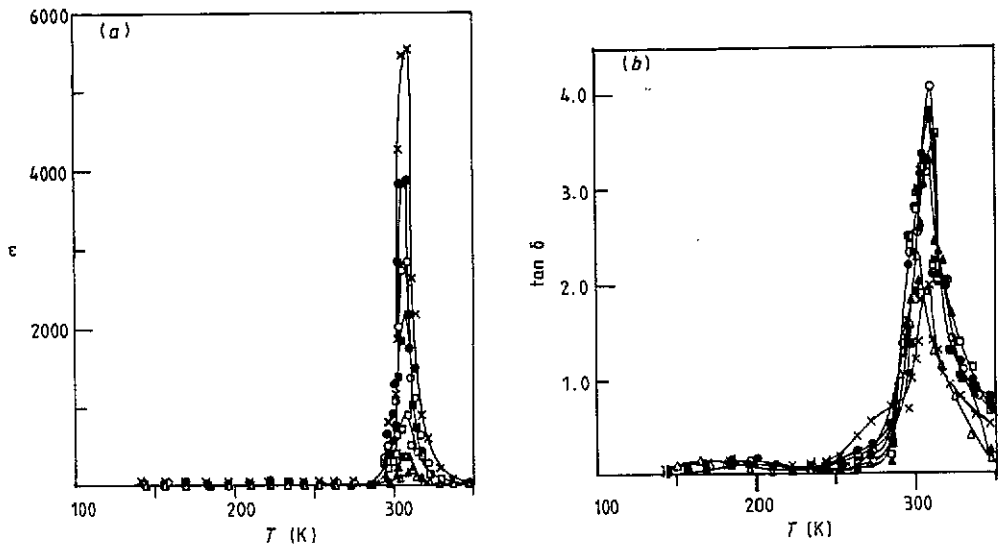


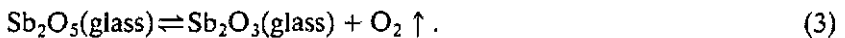
Figure 7. (a) Variation in dielectric constant as a function of temperature for glass 2: \times , 2 kHz; \bullet , 5 kHz; \circ , 7 kHz; \blacksquare , 10 kHz; \square , 20 kHz; \blacktriangle , 50 kHz; \triangle , 100 kHz. (b) Variation in $\tan \delta$ as a function of temperature for glass 2: \times , 2 kHz; \bullet , 5 kHz; \circ , 7 kHz; \blacksquare , 10 kHz; \square , 20 kHz; \blacktriangle , 50 kHz; \triangle , 100 kHz.

Table 3. Parameters obtained from the CBH model by least-squares fitting in the temperature range 170–290 K

Glass	τ_0 (s)	W_M (eV)	R_ω (Å)	N_t (cm ⁻³)
1	1×10^{-13}	0.68	51	9.3×10^{17}
2	3×10^{-13}	0.66	51	1.1×10^{18}

4. Discussion

The first pronounced minimum in the AC resistivity observed in both the glasses at around 310 K is ascribed to the following reaction:



This conclusion is based on the fact that the $[\text{Sb}^{5+}]/[\text{Sb}^{3+}]$ ratio is reduced drastically on heating the glasses to a temperature of 353 K, as shown in table 2. Similar results were confirmed earlier for melt-quenched silicate glasses containing antimony oxide (Chakravorty *et al* 1979). It should be noted that the AC resistivity variation with temperature in the range 280–330 K can be reproduced during the cooling cycle of measurement only after holding the sample at these temperatures for a period of about 100 h. This indicates that the reaction mentioned above is asymmetrical in nature.

The nature of the variation in s as a function of temperature in the range 170–290 K appears to conform to that characteristic of the correlated-barrier hopping (CBH) model (Elliott 1987). We therefore apply this model with two electrons hopping simultaneously between the defect sites in the present case. The latter consist of the Sb^{3+} and Sb^{5+} sites, respectively. The AC resistivity in this model is given by

$$\rho(\omega) = 12/\pi^3 N^2 \epsilon \epsilon_0 \omega R_\omega^6 \quad (4)$$

where N is the spatial density of localized states, ϵ the dielectric constant of the glass, ϵ_0 the free-space permittivity, ω the angular frequency and R_ω the hopping length. The latter is given by

$$R_\omega = 2e^2/\pi \epsilon \epsilon_0 [W_M + kT \ln(\omega \tau_0)] \quad (5)$$

where e is the electronic charge, W_M the barrier height at infinite intersite separation, k the Boltzmann constant, T the temperature and τ_0 a characteristic relaxation time of the order of inverse phonon frequency. The frequency exponent s is expressed by

$$s = 1 - 6kT/[W_M + kT \ln(\omega \tau_0)]. \quad (6)$$

We have attempted to fit the experimental results in the temperature range under consideration using W_M and τ_0 as parameters. It has not been possible to obtain a close fit although the calculated values show the correct trend. The least-squares fitted curves are shown in figures 4 and 5 and values obtained for the different parameters are summarized in table 3. It is evident that the fraction of antimony ion sites contributing to AC conduction according to the CBH model is small, a typical value being 10^{-3} .

From the nature of the variation in s as a function of temperature in the range 100–170 K it appears that the overlapping large-polaron (OLP) tunnelling mechanism could be operative here (Long 1982). In this case the polarons have a spatial extent which is large compared with the interatomic spacing. According to this model the polaron

Table 4. Parameters obtained from the OLP model by least-squares fitting in the temperature range 100–170 K.

Glass	W_{H0} (eV)	r_0 (Å)	α (Å ⁻¹)	R_ω (Å)	$N(E_F)$ (eV ⁻¹ cm ⁻³)
1	0.12	3.8	0.50	12.6	1.4×10^{23}
2	0.10	4.0	0.49	16.2	8.9×10^{22}

hopping energy W_H is given by

$$W_H = W_{H0}(1 - r_0/R) \quad (7)$$

where r_0 is the large-polaron radius, W_{H0} is a constant and R is the intersite distance.

The AC resistivity can be expressed as follows:

$$\rho(\omega) = 12(2\alpha kT + W_{H0} r_0/R_\omega^2)/\pi^4 e^2 (kT)^2 [N(E_F)]^2 \omega R_\omega^4 \quad (8)$$

where α^{-1} is the spatial decay constant for the localized electron wavefunction, $N(E_F)$ the density of localized states at the Fermi level and R_ω the tunnelling distance at angular frequency ω which is given by

$$R_\omega = (1/4\alpha) \{ [\ln(1/\omega\tau_0) - W_{H0}/kT] + \sqrt{[\ln(1/\omega\tau_0) - W_{H0}/kT]^2 + 8\alpha r_0 W_{H0}/kT} \}. \quad (9)$$

The frequency exponent s can be calculated from the following equation:

$$s = 1 - (8R_\omega \alpha + 6r_0 W_{H0}/R_\omega kT)/(2R_\omega \alpha + r_0 W_{H0}/R_\omega kT)^2. \quad (10)$$

We have tried to fit the experimental data on s by a least-squares method in the temperature interval 100–170 K using W_{H0} , r_0 and α as parameters. The theoretical curves for glasses 1 and 2 are shown in figures 4 and 5, respectively. The fit is not good but the calculated values give the correct trend of variation for s as a function of temperature. It should be noted that the theoretical fit to experimental data is much better for glass 1 than for glass 2. In the latter case the maximum value of s is found to be larger than unity. It is likely that in that sample which contains a large amount of antimony ions there are antimony-rich clusters present within the matrix besides the antimony-rich laminae as discussed below. This gives rise to an extra space charge relaxation, thereby making the theoretical fit worse for glass 2 than for glass 1. The values of the parameters obtained by the fitting procedure are summarized in table 4. The number of antimony sites participating in the OLP mode of conduction can be estimated from $kTN(E_F)$ with $T = 170$ K. From the calculated $N(E_F)$ -values we find this number to be equal to 2.1×10^{21} cm⁻³ and 1.3×10^{21} cm⁻³ for glasses 1 and 2, respectively. These are of the same order as the antimony concentration present in these glasses as estimated from chemical analysis and shown in table 1. Comparing these values of N_i with those determined from the CBH model, it is evident that most of the antimony sites contribute to AC resistivity by the OLP tunnelling mechanism. This also implies that the glasses have regions probably in laminar form having antimony-rich and antimony-deficient phases. Because of the series configuration of these layers the region having a higher resistance value would control the overall resistivity change in a particular temperature interval.

In view of the conclusion drawn above regarding the presence of antimony-rich and antimony-deficient layers in the present glass system, the high value of dielectric constant

at around 310 K is believed to arise because of the space charge polarization occurring at the interface between them. The effect is similar to that exhibited by barrier layer capacities where the barrier layers are formed at the interface between semiconducting grains and insulating grain boundaries (Wernicke 1981). However, it should be noted that in the present system the tails of the relevant curves arise owing to the conversion of Sb^{5+} ions to the Sb^{3+} state as the temperature is increased.

5. Conclusions

AC resistivities as a function of temperature of sol-gel-derived glasses in the system $\text{Sb}_2\text{O}_3-(1-x)\text{SiO}_2$ with $x = 0.07$ and 0.23 show two minima at temperatures of around 310 K and 190 K, respectively. The first minimum which is sharp arises because of a chemical reaction involving the conversion of Sb^{5+} ions to Sb^{3+} ions as the temperature is increased. The frequency exponent s shows a maximum at 178 K and 209 K, respectively, for the two glasses. The trend of s variation can be explained by using CBH and OLP models in the higher and lower temperature changes respectively. The calculated values of the antimony site concentration as deduced from these models imply that there are antimony-rich and antimony-deficient layers present in the glass system. An anomalously large value of dielectric constant in the range 1000–6000 at a frequency of 2 kHz at around 310 K appears to corroborate such a distribution of antimony ions.

Acknowledgment

A Datta thanks the Council of Scientific and Industrial Research, Government of India, for the award of a research fellowship. The work has also been supported by a grant from the National Science Foundation, Washington, USA, through the special Foreign Currency Programme.

References

- Chakravorty D, Kumar D and Sastry G V S 1979 *J. Phys. D: Appl. Phys.* **12** 2209
- Close P, Shepherd H M and Drummond C H 1958 *J. Am. Ceram. Soc.* **41** 455
- Datta A, Giri Anit K and Chakravorty D 1991 *Appl. Phys. Lett.* **59** 414
- Elliott S R 1987 *Adv. Phys.* **36** 135
- Hirashima H, Watanabe Y and Yoshida T 1987 *J. Non-Cryst. Solids* **95–6** 825
- Kumar D and Chakravorty D 1980 *J. Phys. D.: Appl. Phys.* **13** 1331
- Long A R 1982 *Adv. Phys.* **31** 553
- Murawski L, Chung C H and McKenzie J D 1979 *J. Non-Cryst. Solids* **32** 91
- Vogel A I 1978 *Textbook of Quantitative Inorganic Analysis* (New York: Longmans) p 383
- Warnicke R 1981 *Grain Boundary Phenomenon in Electronic Ceramics* vol 1, ed L H Levinson (Columbus, OH: American Ceramic Society) p 261